



Plasmon-Enhanced Photocathode for High Brightness and High Repetition Rate X-Ray Sources

A. Polyakov,* C. Senft, K. F. Thompson, J. Feng, S. Cabrini, P. J. Schuck, and H. A. Padmore
LBNL, 1 Cyclotron Road, Berkeley, California 94720, USA

S. J. Peppernick and W. P. Hess
PNNL, 902 Batelle Boulevard, Richland, Washington 99352, USA
(Received 6 November 2012; published 11 February 2013)

In this Letter, we report on the efficient generation of electrons from metals using multiphoton photoemission by use of nanostructured plasmonic surfaces to trap, localize, and enhance optical fields. The plasmonic surface increases absorption over normal metals by more than an order of magnitude, and due to the localization of fields, this results in over 6 orders of magnitude increase in effective nonlinear quantum yield. We demonstrate that the achieved quantum yield is high enough for use in rf photoinjectors operating as electron sources for MHz repetition rate x-ray free electron lasers.

DOI: [10.1103/PhysRevLett.110.076802](https://doi.org/10.1103/PhysRevLett.110.076802)

PACS numbers: 73.20.Mf, 41.60.Cr, 78.67.-n, 79.60.Jv

High brightness electron sources are at the heart of a new generation of x-ray sources based on the free electron laser (FEL) [1], as well as in energy recovery linac and inverse Compton scattering sources [2]. The source of electrons consists of a photoinjector composed of a laser-driven photocathode in a high gradient electric field produced by a rf cavity. The function of the rf cavity is to provide a field sufficient for acceleration of electrons to relativistic velocity over a small distance, thus minimizing the effects of space charge. Even so, the dense electron beam required for high brightness suffers from a space charge field that chirps and reshapes the electron pulse, increasing beam emittance, and thus reducing the overall brightness [3]. This emittance growth can be avoided if the initial distribution of electrons is pancake shaped [4], with a semi-circular transverse intensity profile. In this case, the electron distribution develops under its space charge field from a pancake into a uniformly filled ellipsoidal bunch [5]. This condition, referred to as the blowout regime, requires ultrashort pulses less than 100 fs long and has been successfully demonstrated recently in a high gradient photoinjector [6].

The UV light normally used for photoinjector applications is typically produced by nonlinear crystal-based third harmonic generation using light from a Ti:sapphire 800 nm laser. By choosing a metal cathode with a work function close to the photon energy, the resulting electron beam has only a fraction of an electron volt energy spread as required for low emittance applications [7]. However, in this regime metals have low quantum efficiency, typically on the order of 10^{-5} , which—combined with the losses in the harmonic generation and UV optics—requires the use of pulse energies as high as 1 mJ in order to generate sufficient charge. It has recently been demonstrated that such high pulse energies in the blowout regime yield a higher effective quantum efficiency if the fundamental 800 nm IR laser wavelength is used in a three-photon photoemission process rather

than up-converting to the UV [8]. Additionally, the use of IR-based multiphoton photoemission will significantly simplify the laser system, allowing a more robust and precise beam intensity shaping. The fundamental problem with using IR wavelengths for multiphoton photoemission lies in the intrinsically high reflectivity of metals (over 96% at 800 nm for the noble metals [9]). In this Letter, we show how metal reflectivity is reduced to below 1% by use of a subwavelength nanostructure that completely traps light, resulting in over 6 orders of magnitude increase in the nonlinear electron yield.

The light trapping nanostructure design is based on a theoretical concept proposed by Le Perchec *et al.* [10], where a set of rectangular grooves arranged in a subwavelength array, Fig. 1(a), was predicted to completely absorb light on the metal surface anywhere from the UV to the IR. This light trapping effect has been investigated for a range of geometries by other groups (for example, see Ref. [11]) and was recently demonstrated in our optical work [12]. Each groove acts as a plasmonic resonance nanocavity (NC) with the on-resonance field distribution as shown in Figs. 1(b) and 1(c). The maximum electric field is at the mouth of the NC for enhancing the photoemission. Collectively, the NCs make up a surface impedance matched structure for efficient coupling between the incident light polarized perpendicular to the array in the x direction (p polarization) and the surface plasmon polariton (SPP) resonant mode within the NC [13]. The structure is produced by electron-beam (e -beam) lithography as described in Ref. [14] (the metal is e -beam evaporated on the template and then stripped to produce NCs 15 nm wide and 60 nm deep set with a 100 nm period). In this work, the resonance was chosen around 720 nm with the NC dimensions designed to yield a large spectral bandwidth as shown in Fig. 2(a). A finite-difference time domain (FDTD) calculation is in good agreement with experiment, showing a remarkable on-resonance reflectivity reduction

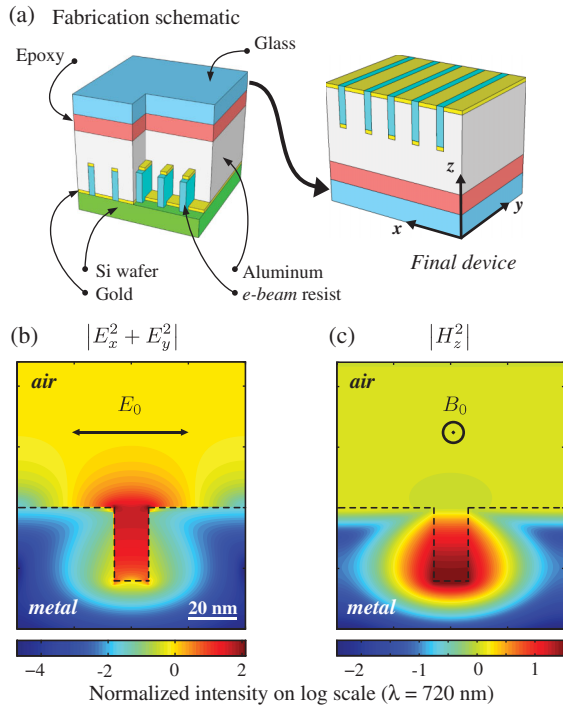


FIG. 1 (color). A set of nanocavities (NCs) were fabricated from a template produced by electron beam lithography (a). FDTD simulations show that the NCs cause an order of magnitude electric field enhancement at the mouth of the NC (b) and in magnetic field at the base of the NC (c). Light is normal to the surface with the electric vector perpendicular to the cavity axis (p polarization).

to below 1%. An absorption enhancement measured at shorter wavelengths is attributed to the surface roughness [15] not included in the FDTD model. Light polarized along the NC array in the y direction (s polarization) cannot couple to the NC SPPs and the reflectivity of an unstructured metal is observed; see the optical image of Fig. 2(a) showing the dramatic reflectivity contrast between the s and p polarization. The effect of the NC array is threefold: complete light absorption, field localization due to short plasmon skin depth, and field enhancement leading to an electron emission with a controllable spatial distribution that could be useful in a range of applications, such as in the realization of a recently proposed superradiant inverse Compton scattering source [2].

Because of the uncertainty principle, the ultrashort pulses of a few tens of fs required for the blowout regime have a large spectral bandwidth—over 100 nm for a 20 fs pulse at 800 nm center wavelength. The NC cathode is an ideal metallic absorber with over 350 nm spectral bandwidth and additionally benefiting from a large angular bandwidth of over 75 deg—defined as the FWHM in the angle of the on-resonance reflectivity dip; see Fig. 2(b). This allows for the use of large aperture focusing for producing a small optical beam size. In this case, unlike in the grating coupled or Kretschmann systems [16], large

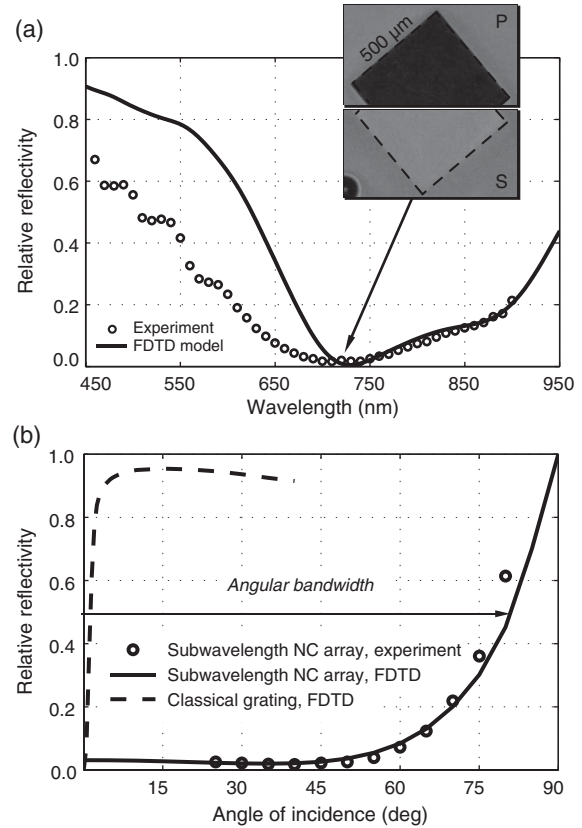


FIG. 2. Optical response of the plasmon-enhanced cathode. Experimentally determined spectral bandwidth, in good agreement with the FDTD simulation, shows broadband response with an on-resonance (720 nm) reflectivity less than 1% (a). The inset shows an optical image of the patterned area demonstrating the large absorption increase from s - to p -polarized normal incidence illumination. Unlike a classical grating, the coupling to the resonant plasmon modes inside the nanocavities leads a very wide angular bandwidth (b).

numerical aperture ($= 1$) optics can be used to produce a wavelength limited focus if required, and still the structure will absorb the majority of the incident radiation over a large spectral bandwidth.

The photoemitted electrons from the NC structure were imaged in a photoemission electron microscope (PEEM), a device that uses a set of electromagnetic lenses to produce a high magnification image of the photoemission pattern [17]. The sample was illuminated by a broadband UV source or by an 800 nm, 60 fs, 90 MHz p -polarized Ti:sapphire laser focused onto a 100 μm diameter spot. To generate a low aberration electron image of the sample, the electromagnetic immersion objective lens has to be placed in close proximity to the sample surface and restrict incidence angle to 75 deg or greater. When illuminated with UV light (far from the nanostructure absorption resonance) the number of electrons produced in a one-photon process was found to be the same for both a structured and an unstructured surface, as shown in Fig. 3(a). Switching the

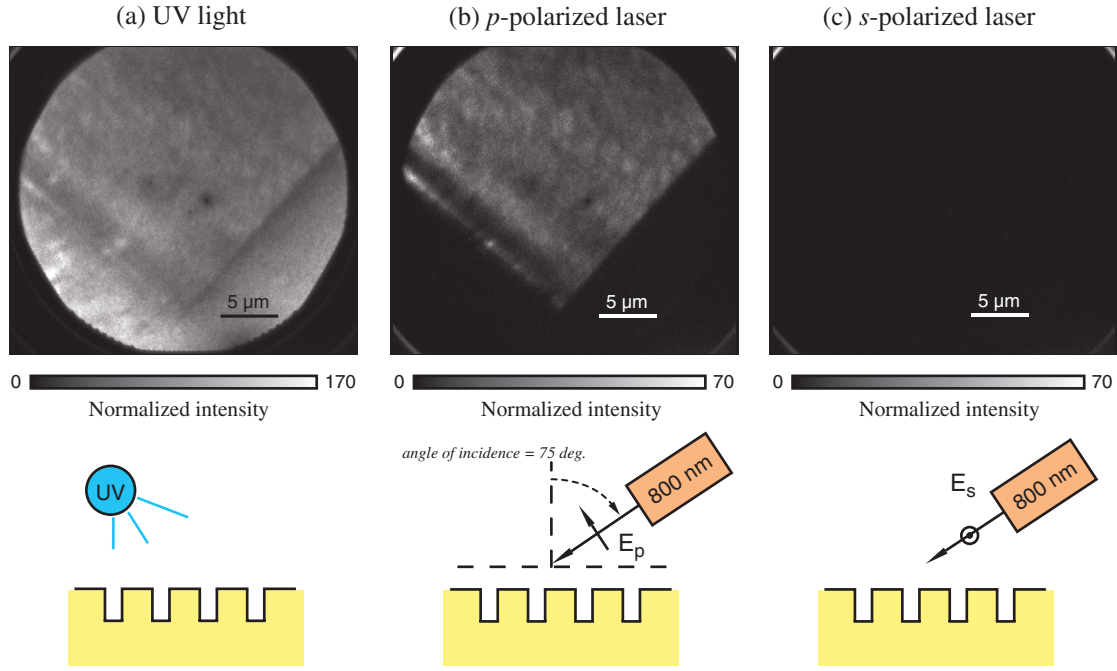


FIG. 3 (color). Plasmonic cathode multiphoton photoemission enhancement imaged in the PEEM. The NC array is prepared on a flat metal substrate which photoemits under UV radiation (a). When illuminated only by an 800 nm laser in p polarization at 75 deg angle of incidence (b) light couples to the plasmonic NCs producing resonant absorption and field enhancement, which leads to a dramatic increase in the multiphoton photoemission producing a bright image only in the patterned area. s -polarized light, however, does not couple to the plasmonic modes and yields the same photocurrent as the flat surface (c). The contrast between the light and the dark area normalized intensity with subtracted background in (b) represents the photoemission enhancement.

illumination to the resonant 800 nm p -polarized light—Fig. 3(b)—produces a large contrast between the pattern and the substrate due to the resonant SPP coupling. This contrast disappears with the electric field of the incident light rotated to s polarization—Fig. 3(c)—consistent with the optical measurements. The dramatic contrast in multiphoton photoemission from the pattern and the substrate demonstrates the enhancement gained by light trapping and the field localization within the NCs.

According to the simplified Fowler-DuBridge model [8,18,19], multiphoton photoemission current density scales as the incident light intensity to the n th power, where n is the order of the photoemission. Because of the limited dynamic range of the PEEM detection system, the emission scaling with power density was quantified in a separate experiment. The sample was placed in a vacuum chamber and illuminated with a 62 MHz 805 nm (1.54 eV) Ti:sapphire laser with 60 fs pulse length focused on a 160 μm diameter spot. The emission current was then measured by an electrometer connected between the sample and the chamber walls:

$$j_n \propto (1 - R)^n I^n A_{\text{spot}},$$

where j_n is the photoemission current density, R is the sample reflectivity, I is the laser intensity, and A_{spot} is the laser spot size. On a log-log plot the current density is expected to scale linearly with the laser intensity with the

slope indicating the photoemission order. A straight line fit shown in Fig. 4 yields $n = 4.01 \pm 0.01$, corresponding to a four-photon photoemission process. The inset shows the photocurrent polarization dependence: at 0 deg the electric field is oriented perpendicular to the NCs (as in Fig. 1), resulting in strong plasmon coupling; as the E vector is rotated by a half wave plate, the sample's absorption decreases with a $[\cos^2(\theta)]^4$ dependence, as expected for a four-photon photoemission process. Because of the short electron mean free path in metals, the photoemission is expected to come predominantly from the top 3 nm thick gold layer (5.3 eV work function [20]) of the nanostructure (see Fig. 1), not the underlying aluminum substrate. Therefore, for the 1.54 eV photons used, only the four-photon process can be observed, in agreement with our experiment.

To prevent sample damage, limited by the thermal conduction of epoxy, the maximum laser intensity used at the pattern was set at $I_{\text{NC}} = 0.065 \text{ GW/cm}^2$, yielding photocurrent $i_{\text{NC}} = 2.45 \text{ pA}$. On the flat metal surface a higher laser intensity of $I_{\text{FS}} = 0.65 \text{ GW/cm}^2$ was used to achieve a maximum photocurrent of $i_{\text{FS}} = 5 \text{ fA}$, in agreement with measurements of the nonlinear yield from a flat gold surface [21]. The fourth-order photoemission enhancement can be expressed as $\eta \equiv (i_{\text{NC}}/I_{\text{NC}}^4)/(i_{\text{FS}}/I_{\text{FS}}^4)$. Using these values the nonlinear yield enhancements from the patterned area was $\eta = 5 \times 10^6$.

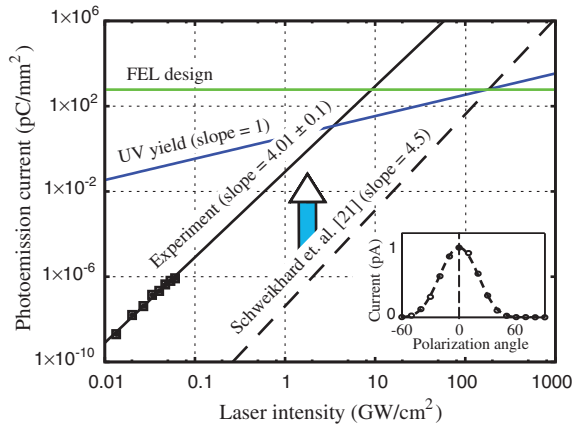


FIG. 4 (color). Experimentally determined photoemission current as a function of laser intensity from the NC array plotted on a log-log scale. Linear fit to the data yields a fourth order photoemission scaling and an enhancement over a flat surface (Schweikhard *et al.* [21]) of more than 6 orders of magnitude. At the pulse charges required, the multiphoton process is shown to be more efficient than the one-photon process (UV). The inset shows the polarization dependence of the photocurrent where 0 deg corresponds to E vector oriented in p polarization (along the x axis); the max-to-min ratio corresponds to the plasmonic photoemission enhancement.

This result can now be scaled to higher pulse charges by using higher laser intensities. As has been experimentally shown by Schweikhard *et al.* in Ref. [22], at intensities up to 50 GW/cm² photoemission is predominantly a multiphoton process. In the space charge limit [23], a 1 μ J (1 W at 1 MHz) 800 nm, 10 fs pulse and a 70 MV/m extraction field would yield a pulse charge:

$$Q_{\text{pulse}}^{\text{max}} = \left(\frac{i_{\text{NC}}}{62 \text{ MHz}} \right)^{1/5} \left(\frac{\epsilon_0 70 \text{ MV/m } 1 \text{ W}}{I_{\text{NC}} 10 \text{ fs } 1 \text{ MHz}} \right)^{4/5} = 0.32 \text{ nC}.$$

The more than 6 orders of magnitude yield enhancement achieved allows us to satisfy the requirements of modern FEL designs [24] at laser intensities below the metal's ablation threshold [25]. Moreover, the modest pulse energy required allows operation at MHz repetition rates using conventional watt-class Ti:sapphire regenerative amplifiers. Additionally, the transverse modulation of the in-phase emitted charge can also be used through emittance exchange [26] in the design of compact superradiant x-ray sources [2].

In summary, we have demonstrated over 6 orders of magnitude fourth-order photoemission enhancement, by use of a subwavelength plasmonic photocathode nanostructure. By nanoengineering the metal surface, a new level of control can be achieved over the resonance wavelength, spectral bandwidth, and angular bandwidth. This can be used to optimally couple femtosecond laser pulses to the surface of a metal in order to achieve efficient operation as an ultrafast MHz repetition rate photocathode. Because of the high quantum efficiency and fast temporal

response of the NC cathode, it has the properties of an ideal photocathode for operation in a MHz-class high brightness x-ray source.

The authors thank M. Zolotarev, P. Musumeci, and R. W. Falcone for useful discussion. S. J. P. and W. P. H. acknowledge support from U.S. Department of Energy Basic Energy Sciences, Division of Chemical Sciences, Geosciences, and Biosciences. Portions of this work were performed as a User project at the Molecular Foundry, Lawrence Berkeley National Laboratory, which is supported by the Office of Science, Office of Basic Energy Sciences, of the U.S. Department of Energy under Contract No. DE-AC0205CH11231.

Note added.—The practical application of a plasmonic photocathode in an rf photogun has been recently demonstrated [27].

*apolyakov@lbl.gov

- [1] W. Ackermann *et al.*, *Nat. Photonics* **1**, 336 (2007).
- [2] W. S. Graves, F. X. Kärtner, D. E. Moncton, and P. Piot, *Phys. Rev. Lett.* **108**, 263904 (2012).
- [3] D. H. Dowell, I. Bazarov, B. Dunham, K. Harkay, C. Hernandez-Garcia, R. Legg, H. Padmore, T. Rao, J. Smedley, and W. Wan, *Nucl. Instrum. Methods Phys. Res., Sect. A* **622**, 685 (2010).
- [4] L. Serafini, in *Towards the X-Ray Free Electron Laser*, edited by R. Bonifacio and W. A. Barletta, AIP Conf. Proc. No. 413 (AIP, New York, 1997), p. 321.
- [5] O. J. Luiten, S. B. van der Geer, M. J. de Loos, F. B. Kiewiet, and M. J. van der Wiel, *Phys. Rev. Lett.* **93**, 094802 (2004).
- [6] P. Musumeci, J. T. Moody, R. J. England, J. B. Rosenzweig, and T. Tran, *Phys. Rev. Lett.* **100**, 244801 (2008).
- [7] D. H. Dowell and J. F. Schmerge, *Phys. Rev. ST Accel. Beams* **12**, 074201 (2009).
- [8] P. Musumeci, L. Cultrera, M. Ferrario, D. Filippetto, G. Gatti, M. S. Gutierrez, J. T. Moody, N. Moore, J. B. Rosenzweig, C. M. Scoby, G. Travish, and C. Vicario, *Phys. Rev. Lett.* **104**, 084801 (2010).
- [9] P. B. Johnson and R. W. Christy, *Phys. Rev. B* **6**, 4370 (1972).
- [10] J. L. Percec, P. Quémerais, A. Barbara, and T. López-Ríos, *Phys. Rev. Lett.* **100**, 066408 (2008).
- [11] K. Aydin, V. E. Ferry, R. M. Briggs, and H. A. Atwater, *Nat. Commun.* **2**, 517 (2011).
- [12] A. Polyakov, S. Cabrini, S. Dhuey, B. Harteneck, P. J. Schuck, and H. A. Padmore, *Appl. Phys. Lett.* **98**, 203104 (2011).
- [13] A. Polyakov, M. Zolotarev, P. J. Schuck, and H. A. Padmore, *Opt. Express* **20**, 7685 (2012).
- [14] A. Polyakov, H. A. Padmore, X. Liang, S. Dhuey, B. Harteneck, J. Schuck, and S. Cabrini, *J. Vac. Sci. Technol. B* **29**, 06FF01 (2011).
- [15] H. Raether, *Surface Plasmons on Smooth and Rough Surfaces and on Gratings* (Springer-Verlag, Berlin, 1988).
- [16] J. Homola, S. Yee, and G. Gauglitz, *Sensor. Actuator. B Chem.* **54**, 3 (1999).

- [17] S. Anders, H. A. Padmore, R. M. Duarte, T. Renner, T. Stammler, A. Scholl, M. R. Scheinfein, J. Stohr, L. Seve, and B. Sinkovic, *Rev. Sci. Instrum.* **70**, 3973 (1999).
- [18] R. Fowler, *Phys. Rev.* **38**, 45 (1931).
- [19] L. DuBridge, *Phys. Rev.* **43**, 727 (1933).
- [20] J. Riviere, *Appl. Phys. Lett.* **8**, 172 (1966).
- [21] V. Schweikhard, A. Grubisic, T. A. Baker, and D. J. Nesbitt, *J. Phys. Chem. C* **115**, 83 (2011).
- [22] V. Schweikhard, A. Grubisic, T. A. Baker, I. Thomann, and D. J. Nesbitt, *ACS Nano* **5**, 3724 (2011).
- [23] Á. Valfells, D. W. Feldman, M. Virgo, P. G. O'Shea, and Y. Y. Lau, *Phys. Plasmas* **9**, 2377 (2002).
- [24] W. A. Barletta *et al.*, *Nucl. Instrum. Methods Phys. Res., Sect. A* **618**, 69 (2010).
- [25] V. K. Valev *et al.*, *Adv. Mater.* **24**, OP208 (2012).
- [26] M. Cornacchia and P. Emma, *Phys. Rev. ST Accel. Beams* **5**, 084001 (2002).
- [27] R. K. Li, H. To, G. Andonian, J. Feng, A. Polyakov, C. M. Soby, K. Thompson, W. Wan, H. A. Padmore, and P. Musumeci, *Phys. Rev. Lett.* (to be published).